Transition-metal Complexes of Pyrrole Pigments. Part VI.† Some Bivalent Metal Complexes of 3,3′,4,4′-Tetrachloro-5,5′-diethoxycarbonyldipyrromethene

By **Yukito Murakami,* Yoshihisa Matsuda,** and **Kazunori Sakata,** Department of Organic Synthesis, Faculty of Engineering, Kyushu University, Fukuoka 812, Japan
Arthur E. Martell, Department of Chemistry, Texas A & M University, College Station, Texas 77843, U.S.A.

The cobalt(II), nickel(II), copper(II), and zinc(II) complexes of 3,3′,4,4′-tetrachloro-5,5′-diethoxycarbonyldipyrromethene were investigated by means of electronic, vibrational, and e.s.r. spectroscopy as well as *X*-ray diffraction measurements of powdered samples. I.r. and visible spectral data proved the distorted tetrahedral co-ordination of $M-N_4$ type for the cobalt(II) and zinc(II) complexes. The nickel(II) and copper(II) complexes showed two kinds of carbonyl bands in their i.r. spectra, and the $d \longrightarrow d$ transition bands were consistent with the distorted octahedral (C_2) co-ordination. E.s.r. spectra of the copper complex were characteristic of rhombic co-ordination, showing $g_1 \simeq g_2 > g_3$ and $A_3 > A_2 \simeq A_1$. Both nickel and copper complexes consequently possess a distorted octahedral configuration of $M-N_4O_2$ type around the central metal atoms. The characteristic features of *X*-ray diffraction patterns for the four metal complexes were consistent with these structural assignments.

FROM our structural investigations on various divalent metal chelates of substituted dipyrromethenes (I),[1-3] cobalt(II) was found to co-ordinate tetrahedrally to dipyrromethene molecules, the dihedral angle between two ligand planes being maintained at nearly 90°, regardless of the nature and bulkiness of the 5,5′-substituents. Such configuration seems to minimize the steric hindrance between such substituents in a molecule. On the other hand, copper(II) tends to co-ordinate with

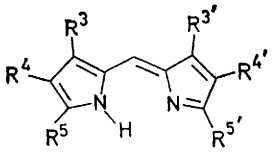

(I)

ligands in a square-planar manner as far as the circumstances allow. The 5,5′-substituents of dipyrromethenes take part in distorting the co-ordination geometry from square-planar configuration towards tetrahedral depending upon their bulkiness. This trend was also verified by a single-crystal *X*-ray diffraction study.[4] A similar trend was also suggested for the nickel(II) complexes in our previous work [2] and the distorted geometry was illustrated by *X*-ray diffraction study.[5]

3,3′,4,4′-Tetrachloro-5,5′-diethoxycarbonyldipyrromethene was adopted as the ligand in this work to form the corresponding metal chelates with Co^{II}, Ni^{II}, Cu^{II}, and Zn^{II}. Different from the previous dipyrromethene ligands, the ethoxycarbonyl groups, which would exhibit co-ordination ability under certain configurational conditions, are placed at the 5,5′-positions in the present ligand. Therefore, the metal-specificity would be expected for the formation of six-co-ordinated metal complexes at a 2 : 1 molar ratio of ligand to metal with participation of the ethoxycarbonyl group as a donor. Although Motekaitis and Martell [6] reported the syntheses of Ca^{II}, Cu^{II}, Ni^{II}, Zn^{II}, and Mn^{II} chelates with 3,3′,4,4′-tetrachloro- and 3,3′,4,4′-tetrabromo-5,5′-diethoxycarbonyldipyrromethene ligands as well as their structural investigations by electronic, i.r., and n.m.r. spectroscopy, the co-ordination behaviour of the former ligand with particular attention to the ethoxycarbonyl group and the structures of the resulting metal chelates were investigated in more detail in this work through the measurements of their ligand-field bands, e.s.r., and i.r. spectra, and *X*-ray diffraction patterns in powdered sample state.

EXPERIMENTAL

Metal Chelates.—All the metal chelates were prepared by metal–metal exchange reactions performed on the Ca^{II} chelate. Syntheses of bis(3,3′,4,4′-tetrachloro-5,5′-diethoxycarbonyldipyrromethenato)calcium(II), -nickel(II), -copper(II), and -zinc(II) were carried out by the methods described previously [6] (Found: C, 39·55; H, 2·55; N, 6·2. Calc. for $C_{30}H_{22}N_4O_8Cl_8Ni$: C, 39·65; H, 2·45; N, 6·15. Found: C, 39·4; H, 2·6; N, 6·05. Calc. for $C_{30}H_{22}N_4O_8Cl_8Cu$: C, 39·45; H, 2·45; N, 6·15. Found: C, 39·6; H, 2·6; N, 6·2. Calc. for $C_{30}H_{22}N_4O_8Cl_8Zn$: C, 39·35; H, 2·4; N, 6·1%).

Bis(3,3′,4,4′-tetrachloro-5,5′-diethoxycarbonyldipyrromethenato)cobalt(II) was prepared in a similar manner. A mixture of bis(3,3′,4,4′-tetrachloro-5,5′-diethoxycarbonyldipyrromethenato)calcium(II) (0·32 g) and cobalt(II) acetate tetrahydrate (0·11 g) was refluxed in absolute ethanol (750 ml) for 4 h. After the reaction mixture being allowed to stand overnight at room temperature, the solvent was removed under vacuum. The residue was extracted into hot benzene and again the solvent was removed under reduced pressure. The remaining solid material was extracted into hot n-pentane. Bright green prism-like crystals were obtained; yield 0·23 g (70%) (Found: C, 39·8; H, 2·6; N, 6·15. Calc. for $C_{30}H_{22}N_4O_8Cl_8Co$: C, 39·65; H, 2·45; N, 6·15%).

Spectra.—Electronic spectra in chloroform were recorded on a Hitachi EPS 2 spectrophotometer at room temperature. I.r. spectra were measured with a JASCO

† Part V, ref. 3.

[1] Y. Murakami and K. Sakata, *Inorg. Chim. Acta*, 1968, **2**, 273.
[2] Y. Murakami, Y. Matsuda, and K. Sakata, *Inorg. Chem.*, 1971, **10**, 1728.
[3] Y. Murakami, Y. Matsuda, and K. Sakata, *Inorg. Chem.*, 1971, **10**, 1734.
[4] M. Elder and B. R. Penfold, *J. Chem. Soc.* (*A*), 1969, 2556.
[5] F. A. Cotton, B. G. DeBoer, and J. R. Pipal, *Inorg. Chem.*, 1970, **9**, 783.
[6] R. J. Motekaitis and A. E. Martell, *Inorg. Chem.*, 1970, **9**, 1832.

DG 403 G spectrophotometer at room temperature in chloroform as well as by a Nujol mull technique. E.s.r. spectra of the copper chelate were recorded on a JEOL JES ME 3 spectrometer equipped with a 100 kHz field modulation unit, and either with *X*-band or *K*-band microwave unit. The sample was measured in xylene–benzene (6 : 4) at −135° and room temperature. The powdered solid sample was also provided for measurements at room temperature. MgO–Mn(II) was used to establish the standard reference signals for e.s.r. spectra.

X-Ray Diffraction Patterns.—These patterns of the powdered solid samples were measured using a Rigaku Denki SD *X*-ray diffractometer.*

RESULTS

Electronic Spectra.—The electronic spectra of the Co^{II}, Ni^{II}, and Cu^{II} chelates are shown in Figure 1. The absorption bands appearing above 18 000 cm^{-1} are attributed to charge-transfer transitions and $\pi \longrightarrow \pi^*$ transitions within a ligand molecule. Thus, these bands bear a close resemblance among above three metal chelates. The ligand-field bands are observed in a region lying below 18 000 cm^{-1}. These data and the corresponding assignments are listed in Table 1 along with the data for some other dipyrromethene chelates from our previous work [2] for comparison. General features of the ligand-field bands for the present Co^{II} chelate are similar to those for previously studied Co^{II} chelates. These bands for the former chelate bear the closest resemblance in their intensities to the corresponding bands for the 5,5′-diphenyldipyrromethene chelate. The spectral behaviour of the present Ni^{II} chelate is most analogous to that of the 5,5′-diphenyldipyrromethene chelate. However, both bands appearing in 6000—13 000 cm^{-1} shifted toward higher energy region and their relative intensity is somewhat changed for the present chelate. All the ligand-field bands of the present Cu^{II} chelate shifted toward lower energy relative to those of the other dipyrromethene chelates previously studied by us. General features of the spectrum are also somewhat modified from the others and the absorption intensities are significantly lowered.

Vibrational Spectra.—The i.r. spectra of the Co^{II}, Ni^{II}, Cu^{II}, and Zn^{II} chelates are shown in Figure 2 only for the carbonyl frequency region. The Co^{II} and Zn^{II} chelates show a single sharp band due to C=O stretching vibration, while the Cu^{II} and Ni^{II} chelate spectra have two bands. All these chelates show a sharp single absorption attributable to the skeletal stretching mode of the pyrrole rings *ca.* 1600 cm^{-1}.

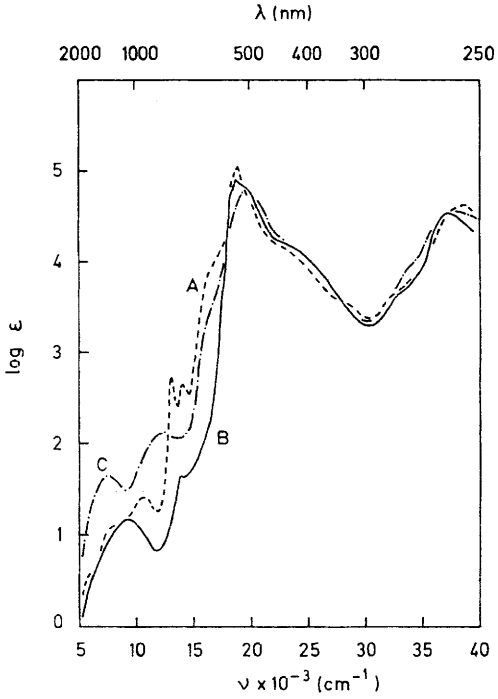

FIGURE 1 Electronic absorption spectra of the 3,3′,4,4′-tetrachloro-5,5′-diethoxycarbonyldipyrromethene chelates in chloroform at room temperature: (A), Co^{II}; (B), Ni^{II}; (C), Cu^{II}

E.s.r. Spectra.—These spectra for the Cu^{II} chelate under various conditions are shown in Figure 3. The solution spectrum at room temperature shows only a single resonance peak, while the e.s.r. spectra for polycrystalline sample and samples in frozen homogeneous solution provide *g*-values of anisotropic nature. A powdered polycrystalline sample furnished the *X*-band e.s.r. spectrum of rhombic character which was further verified by the aid of the corresponding *K*-band spectrum upon evaluation of three *g*-values. The solution spectrum measured at −135° clearly indicates the

TABLE 1

Ligand-field bands for dipyrromethene chelates and their assignments [a,b]

Metal	Ligand [c] (I) [d]	(II) [d]	(III) [d]	(IV)	Assignment D_2	T_d	C_2
Co^{II}	6200sh	6700sh (24)	7800sh (13)	6000sh (3·9)	$B_1 \leftarrow A$		
	8470	8200sh (53)	8800sh (17)	8300sh (13·2)	$B_2 \leftarrow A$	$^4T_1(F) \leftarrow {}^4A_2(F)$	
	10 200sh	10 000 (67)	10 000 (26)	10 500 (26·3)	$B_3 \leftarrow A$		
	13 300	13 200 (336)	12 300 (639)	12 900 (530)	$B_1 \leftarrow A$		
	14 500	14 400 (304)	13 300 (499)	14 000 (426)	$B_2 \leftarrow A$	$^4T_1(P) \leftarrow {}^4A_2(F)$	
	16 500sh	16 900sh (1885)	16 700sh (20 400)	15 900sh (4840)	$B_3 \leftarrow A$		
Ni^{II}	8120 (13)	6300 (26)	6100 (17)	9260 (14·6)		$^3A_2(F) \leftarrow {}^3T_1(F)$	$A,B,A(T_{2g}(F)) \leftarrow A$
		11 000sh (48)					
	11 200 (82)	12 700 (574)	11 800 (759)	13 900 (44·8)			$B,A,B(T_{1g}(F)) \leftarrow A$
	12 930 (143)	13 850 (474)	13 300sh (500)	14 900sh (55·9)		$^3T_1(P) \leftarrow {}^3T_1(F)$	$B,A,B(T_{1g}(P)) \leftarrow A$
	15 600sh (583)	15 000sh (225)	15 900sh (40 500)				
Cu^{II}	12 750sh (132)	10 900 (278)	8850 (456)	7450 (45)	$B_2,B_3 \leftarrow B_1$		$A \leftarrow A$
	14 000sh (165)			12 300 (131)			$B \leftarrow A$
	16 400sh (1320)	16 500sh (1550)	14 700 (2600)	15 900sh (1270)	$A,A' \leftarrow B_1$		$A \leftarrow A$
			15 600 (2490)				

[a] Band positions are expressed in cm^{-1} and molar extinction coefficients are given in parentheses after the band positions. [b] Measured at room temperature in chloroform. [c] (I), 3,3′,4,4′-tetramethyldipyrromethene; (II), 3,3′,5,5′-tetramethyldipyrromethene; (III), 5,5′-diphenyldipyrromethene; (IV), 3,3′,4,4′-tetrachloro-5,5′-diethoxycarbonyldipyrromethene. [d] From ref. 2.

* Measurements of *X*-ray diffraction patterns were carried out at the Research Institute of Yoshitomi Pharmaceutical Co., Ltd., whose courtesy is greatly acknowledged.

relation, $g_1 \simeq g_2 > g_3$, under the measuring condition. In the g_3 position, there consists of nearly equally spaced four

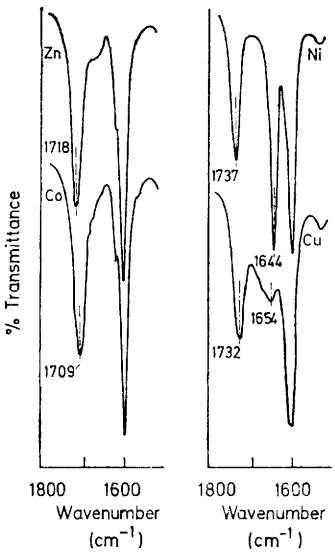

FIGURE 2 I.r. spectra of the 3,3′,4,4′-tetrachloro-5,5′-diethoxycarbonyldipyrromethene chelates in chloroform at room temperature (number refers to the carbonyl stretching band in cm^{-1})

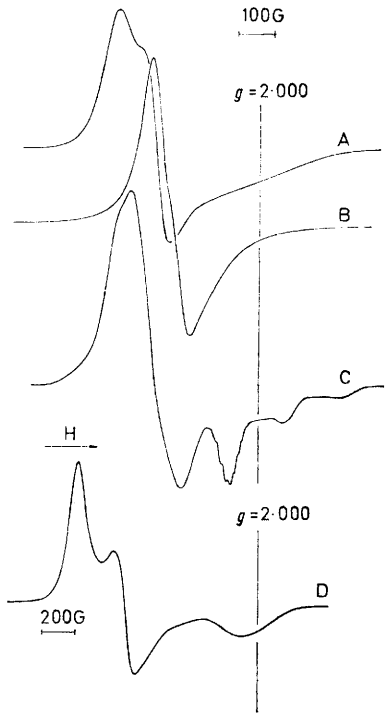

FIGURE 3 E.s.r. spectra of bis(3,3′,4,4′-tetrachloro-5,5′-diethoxycarbonyldipyrromethenato)copper(II): A, powdered sample at room temperature (*X*-band); B, in xylene–benzene (6 : 4) at room temperature (*X*-band); C, in xylene–benzene (6 : 4) at −135° (*X*-band); D, powdered sample at room temperature (*K*-band)

resonance peaks, which may be attributed to the hyperfine interaction with the copper atom ($I = 3/2$). In addition, one of these peaks in lower field has a super-hyperfine structure due to four equivalent nitrogen donor atoms. These characteristic features of e.s.r. spectra for the Cu^{II} chelate seem to predict the compressed-tetragonal stereochemistry around the copper atom.[7,8] All the e.s.r. parameters are summarized in Table 2.

X-Ray Diffraction Data.—These patterns for the Ni^{II}, Cu^{II}, and Zn^{II} chelates are shown in Figure 4. These indicate a close resemblance in the nature of molecular

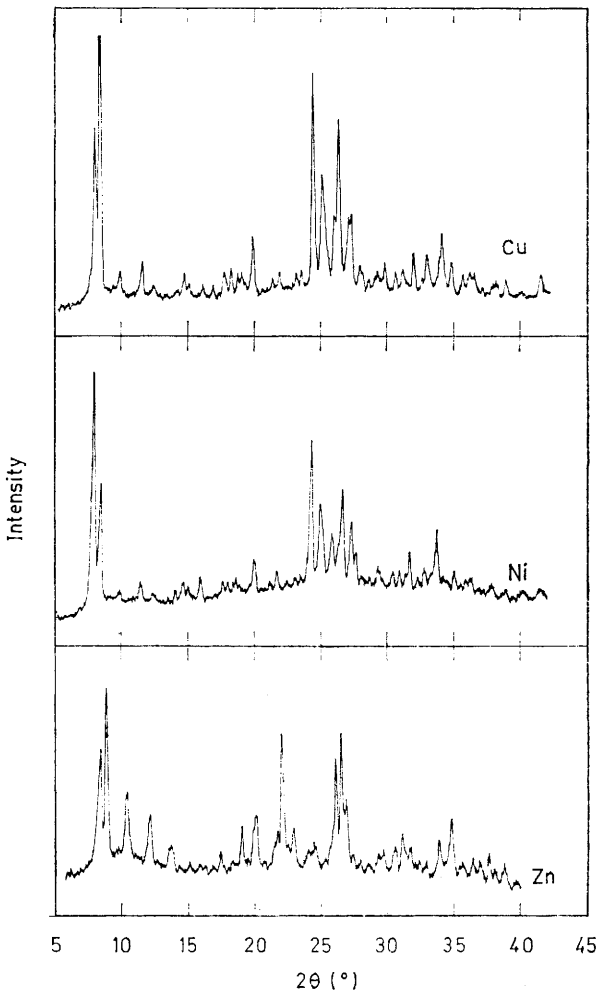

FIGURE 4 *X*-Ray powder diffraction patterns of the 3,3′4,4′-tetrachloro-5,5′-diethoxycarbonyldipyrromethene chelates. The relative diffraction intensity is shown against a Bragg angle θ

packing between the Ni^{II} and Cu^{II} chelates in the solid state, and consequently a similarity in their co-ordination geometry. On the other hand, the diffraction pattern for the Zn^{II} chelate is certainly different from those for the above two chelates. Although the Co^{II} chelate did not provide a well refined pattern due to some crystalline nature, it is certainly not analogous to the patterns for the Ni^{II} and Cu^{II} chelates.

[7] I. M. Procter, B. J. Hathaway, D. E. Billing, R. Dudley, and P. Nicholls, *J. Chem. Soc.* (*A*), 1969, 1192.

[8] R. J. Dosser and A. E. Underhill, *J. Chem. Soc.* (*A*), 1970, 88.

TABLE 2

E.s.r. parameters for bis(3,3',4,4'-tetrachloro-5,5'-diethoxycarbonyldipyrromethenato)copper(II) [a]

Sample	Temp. (°C)	Microwave source	g_1	g_2	g_1'	g_3	$10^4 \times \lvert A_3^{Cu} \rvert$ cm^{-1}	$10^4 \times \lvert A_3^{N} \rvert$ cm^{-1}
Powdered	22	*X*-band	2·280	2·201				
Powdered	22	*K*-band	2·285	2·204		2·204		
Xylene–benzene (6 : 4)solution	22	*X*-band			2·166 [b]			
Xylene–benzene (6 : 4) solution	−135	*X*-band			2·256	2·011	145	11·2

[a] The errors in *g*-values are within ±0·005 and those in *A*-values are less than ±0·1. [b] Averaged *g*-value.

DISCUSSION

Cobalt(II) *and Zinc*(II) *Chelates.*—The i.r. spectrum for the present cobalt chelate indicates that all the ethoxycarbonyl groups in a chelate molecule are placed in space in an equivalent manner. The general feature of the ligand-field spectrum also shows that the cobalt ion is situated approximately in a tetrahedral ligand-field, so that the 5,5'-substituents do not generate any noticeable steric disturbance in a molecule. As a result, the cobalt ion bound to four *N*-donor atoms has a nondegenerate *A* ground state in D_2 symmetry upon some minor distortion from a regular tetrahedron.

Since the Zn^{II} ion has no *d*-electrons in its valence-shell, only i.r. spectrum and *X*-ray diffraction pattern of the chelate provide useful data in the present work for prediction of co-ordination geometry. The zinc chelate has a single carbonyl stretching mode as is the case for the corresponding cobalt chelate. In addition, the *X*-ray diffraction pattern is significantly different from those for the Cu^{II} and Ni^{II} chelates as can be seen from Figure 4. Thus, we believe that the zinc chelate assumes a nearly tetrahedral structure around the metal atom.

Copper(II) *and Nickel*(II) *Chelates.*—The ligand-field bands of the present copper chelate are shifted to lower energy relative to those of the dipyrromethene–Cu^{II} chelates previously studied by us [1,2] and this shift is accompanied by the decrease of absorption intensity. For the dipyrromethene chelates, in which alkyl or phenyl substituents are placed at the 5,5'-positions of a ligand, the dihedral angle between two ligand planes was predicted to increase as the bulkiness of the 5,5'-substituents increases. Consequently, $d \longrightarrow d$ bands shift to lower energy concomitant with the increase of absorption intensity. Therefore, if the distorted tetrahedral co-ordination is still retained for the present copper chelate, the $d \longrightarrow d$ band shift to lower energy must be accompanied with the increase of absorption intensity. The result is contrary to what would be expected for such a case. This suggests that the co-ordination geometry does not belong to D_2 symmetry with $Cu–N_4$ bond type and some other co-ordination configuration comes into play.

The e.s.r. spectrum for the frozen solution gave three *g*-values as $g_1 \simeq g_2 > g_3$. If the co-ordination symmetry is in D_2, these values are expected to be $g_1 > g_2 = g_3$.[3] Furthermore, the i.r. spectrum of the present copper chelate shows the presence of two different types of carbonyl group. On the basis of these facts, the co-ordination geometry around the copper atom may be predicted to be the distorted octahedron with $Cu–N_4O_2$ bonding (II). For models A and B listed in Table 3 (C_{2v} symmetry), the ground state function ψ_A is shown as

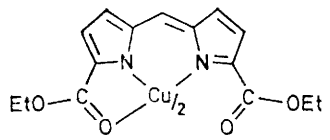

(II)

$\psi_A = d_{z^2}$. Since a g_3-value is somewhat larger than 2·0023, these models cannot be strictly applied to the present system. In addition, the degeneracy of the A_2

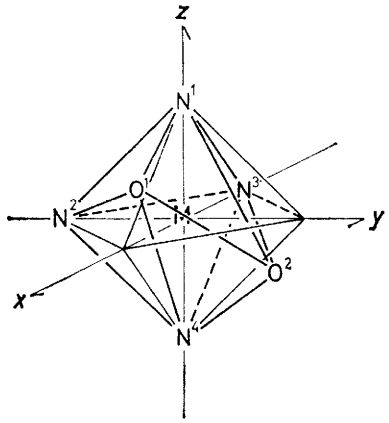

FIGURE 5 Schematic representation of the co-ordination geometry for the copper and nickel chelates (model C) with C_2 symmetry; refer to Table 3 for polar co-ordinates assigned to these point charges. Structure (II) represents the ligand configuration in the copper chelate

TABLE 3

Assignments of constant values to the point charge models

Donor atom	Polar co-ordinate for a point charge [a] r_i	θ_i	ϕ_i	Point charge [b]
N^1	*a*	0		*Ze*
N^2	*a*	π/2	−π/2	*Ze*
N^3	*a*	π/2	π	*Ze*
N^4	*a*	π		*Ze*
O^1	*a'*	θ_0	0	*Z'e*
O^2	*a'*	$\pi - \theta_0$	π/2	*Z'e*

[a] $a = a'$ and $\theta_0 = \pi/2$ for model A; $a \neq a'$ and $\theta_0 = \pi/2$ for model B; $a \neq a'$ and $\theta_0 = \pi/2 + \Delta\theta$ for model C. [b] $Ze > Z'e$. See Appendix for significance.

and B_1 levels does not provide an explanation for the presence of three ligand-field bands. For model C of C_2 symmetry (Figure 5 and Table 3), the ground state function ψ_A is represented as:

$$\psi_A = \alpha d_{z^2} + \beta d_{x^2-y^2} + \gamma/\sqrt{2}(d_{xy} + d_{yz})$$

The Δg_i $(= g_0 - g_i)$ values are given as follows:

$$\Delta g_z = 2\lambda\left[\frac{(\beta\delta - \gamma\zeta)^2}{\Delta E_{B_1}} + \frac{(\beta\tau - \gamma\sigma)^2}{\Delta E_{B_2}}\right]$$

$$\Delta g_x = \Delta g_y = \lambda\left[\frac{(\sqrt{3}\alpha\zeta + \beta\zeta + \gamma\delta)^2}{\Delta E_{B_1}} + \frac{(\sqrt{3}\gamma\kappa - \sqrt{3}\alpha\eta + \beta\eta - \xi\gamma)^2}{\Delta E_{A_2}} + \frac{(\sqrt{3}\sigma\alpha + \beta\sigma + \gamma\tau)^2}{\Delta E_{B_2}} + \frac{(\sqrt{3}\chi\gamma - \sqrt{3}\alpha\omega + \beta\omega - \nu\gamma)^2}{\Delta E_{A_2}}\right]$$

The above equations indicate the relation, $g_1 = g_2 > g_3$, which gives a reasonable explanation for the observed g-values. In addition, three $d \longrightarrow d$ bands observed for the present copper complex may be ascribed to $A \longleftarrow A$, $B \longleftarrow A$, and $A \longleftarrow A$ transitions as seen from Figure 6. The hyperfine coupling constants obtained

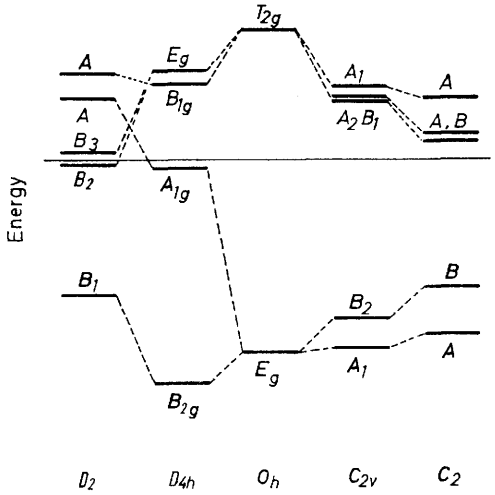

FIGURE 6 Energy levels of the copper(II) ion in the six-co-ordinated complex under various co-ordination symmetries

from e.s.r. study furnished a relation, $A_1 \simeq A_2 < A_3$, which is consistent with the assignments of g-values. In conclusion, the co-ordination configuration of the copper chelate is most plausibly represented by model C (Figure 5).

Although the energy level correlations for various ligand-field symmetries can be shown in Figure 7, the co-ordination stereochemistry of the nickel chelate cannot be predicted on the basis of $d \longrightarrow d$ band assignments alone. The X-ray powder pattern for the nickel chelate is identical enough with that for the corresponding copper chelate as is obvious from Figure 4. The i.r. spectra for both nickel and copper chelates are very

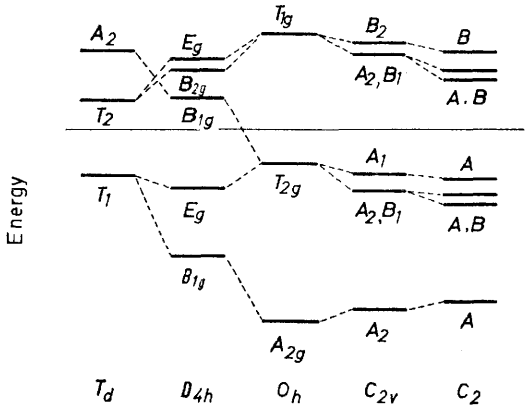

FIGURE 7 Energy levels of the nickel(II) ion in the six-co-ordinated complex under various co-ordination symmetries

much alike, particularly in the carbonyl frequency region. Consequently, the distorted octahedral configuration around the central metal atom (C_2 symmetry) can be assigned to the nickel chelate. The observed ligand-field bands may be attributed to A, B, A (T_{2g}) $\longleftarrow A$, B, A, B $(T_{1g}(F)) \longleftarrow A$, and B, A, B $(T_{1g}(P)) \longleftarrow A$ transitions in an increasing order of energy.

APPENDIX

Calculation of Ligand-Field Splittings.[2]—The point-charge models are established for co-ordination of six donor atoms to a metal as listed in Table 3 to evaluate the energy levels as the molecular site symmetry around the central metal atom is varied. Models A and B belong to C_{2v} symmetry, while model C to C_2.

The ligand-field potential, which arises from the arrangement of six negative charges in space around the central metal ion may be represented by the following equation.

$$V = \sum_{n=2,4}\sum_{m=-n}^{n} A_{nm}r^n Y_{nm}(\theta,\phi)$$

$$A_{nm} = \frac{4\pi}{2n+1}(-1)^m \sum_{i=1}^{6} Z_i e r_i^{-(n+1)} Y_{n-m}(\theta_i,\phi_i)$$

Since terms for $m \neq 2k$ do not become zero for $\theta_0 \neq \pi/2$, the following modification can be adopted.

$$A_{nm}r^n Y_{nm} + A_{n-m}r^n Y_{n-m} = U_{nm}r^n Q_{nm}$$

where U_{nm}-values are represented as follows.

$$U_{20} = (2\sqrt{\pi}/\sqrt{5})ea^{-3}\{Z + (3\cos^2\theta_0 - 1)Z'\rho^{-3}\}$$
$$U_{21} = -(\sqrt{6\pi}/2\sqrt{5})ea^{-3}\sin\theta_0\cos\theta_0 Z'\rho^{-3}$$
$$U_{40} = (\sqrt{\pi}/6)ea^{-5}\{11Z + (35\cos^4\theta_0 - 30\cos^2\theta_0 + 3)Z'\rho^{-5}\}$$
$$U_{41} = -(\sqrt{5\pi}/3)ea^{-5}\{7\cos^3\theta_0 - 3\cos^2\theta_0\}Z'\rho^{-5}$$
$$U_{43} = (\sqrt{35\pi}/3)ea^{-5}\{\sin^3\theta_0\cos^3\theta_0 Z'\rho^{-5}\}$$
$$U_{44} = (\sqrt{35\pi}/6\sqrt{2})ea^{-5}\{Z + \sin^4\theta_0 Z'\rho^{-5}\}$$

with $\rho = a'/a$.

The basis functions are

$$\psi_1 = |0\rangle = d_{z^2}$$
$$\psi_2 = 1/\sqrt{2}(|2\rangle + |\bar{2}\rangle) = d_{x^2-y^2}$$
$$\psi_3 = -i/\sqrt{2}(|2\rangle - |\bar{2}\rangle) = d_{xy}$$
$$\psi_4 = -1/\sqrt{2}(|1\rangle - |\bar{1}\rangle) = d_{xz}$$
$$\psi_5 = i/\sqrt{2}(|1\rangle + |\bar{1}\rangle) = d_{yz}$$

For models A and B, the following eigenvectors are derived.

$$|A_1\rangle = |\psi_1\rangle$$
$$|B_2\rangle = |\psi_2\rangle$$
$$\left.\begin{matrix}|A_2\rangle \\ |B_1\rangle\end{matrix}\right\} = |\psi_4\rangle, |\psi_5\rangle \text{ (degenerate)}$$
$$|A_1\rangle = |\psi_3\rangle$$

For model C with C_2 symmetry (Figure 5), the corresponding eigenvectors are somewhat modified as follows.

$$|A_1\rangle = \alpha|\psi_1\rangle + \beta|\psi_3\rangle + \gamma/\sqrt{2}\{|\psi_4\rangle + |\psi_5\rangle\}$$
$$|B_1\rangle = \delta|\psi_2\rangle + \zeta/\sqrt{2}\{|\psi_4\rangle - |\psi_5\rangle\}$$
$$|A_2\rangle = \eta/\sqrt{2}\{|\psi_4\rangle + |\psi_5\rangle\} + \kappa|\psi_1\rangle + \xi|\psi_3\rangle$$
$$|B_2\rangle = \sigma/\sqrt{2}\{|\psi_4\rangle - |\psi_5\rangle\} + \tau|\psi_2\rangle$$
$$|A_3\rangle = \nu|\psi_3\rangle + \chi/\psi_1\rangle + \omega/\sqrt{2}\{|\psi_4\rangle + |\psi_5\rangle\}$$

The coefficient of the first term in the right hand side of each equation is considered to be largest among others since the θ_0-value does not seem to depart significantly from $\pi/2$. The numbering suffixed to A's and B's simply indicates the relative sequence of energy levels. The energy level splittings and the correlation diagram under various co-ordination site symmetry for the copper(II) chelate are shown in Figure 6.

[2/1845 *Received, 4th August,* 1972]